MPA 1345e

On the helium flash in low-mass Population III Red Giant stars

H. Schlattl[1,2,3], S. Cassisi[2,1], M. Salaris[3,1], A. Weiss[1,4,5]

submitted to: *The Astrophysical Journal*

ABSTRACT

We investigate the evolution of initially metal-free, low-mass Red Giant stars through the He core flash at the tip of the Red Giant Branch. The low entropy barrier between the helium- and hydrogen-rich layers enables a penetration of the helium flash driven convective zone into the inner tail of the extinguishing H-burning shell. As a consequence, protons are mixed into high-temperature regions triggering a H-burning runaway. The subsequent dredge-up of matter processed by He and H burning enriches the stellar surface with large amounts of helium, carbon and nitrogen. Extending previous results by Hollowell et al. (1990) and Fujimoto et al. (2000), who claimed that the H-burning runaway is an intrinsic property of extremely metal-poor low-mass stars, we found that its occurrence depends on additional parameters like the initial composition and the treatment of various physical processes.

We perform some comparisons between predicted surface chemical abundances and observational measurements for extremely metal-deficient stars. As in previous investigations, our results disclose that although the described scenario provides a good qualitative agreement with observations, considerable discrepancies still remain. They may be due to a more complex evolutionary path of 'real' stars, and/or some shortcomings in current evolutionary models.

In addition, we analyze the evolutionary properties after the He core flash, during both the central and shell He-burning phases, allowing us to deduce some interesting differences between models whose Red Giant Branch progenitor has experienced the H-flash and canonical models. In particular, the Asymptotic Giant Branch evolution of extremely metal-deficient stars and the occurrence of thermal pulses are strongly affected by the previous RGB evolution.

Subject headings: stars: abundances — stars: evolution — stars: interiors — stars: late-type

[1]Max-Planck-Institut für Astrophysik, Karl-Schwarzschild-Straße 1, D-85741 Garching, Germany

[2]Osservatorio Astronomico di Collurania, Via M. Maggini, I-64100 Teramo, Italy

[3]Astrophysics Research Institute, Liverpool John Moores University, Twelve Quays House, Egerton Wharf, Birkenhead CH41 1LD, UK

[4]Institute for Advanced Study, Olden Lane, Princeton, USA

[5]Princeton University Observatory, Peyton Hall, Princeton, USA

1. Introduction

The most metal-deficient stars in our Galaxy provide astronomers with a wealth of information about the physical conditions of the universe soon after the Big Bang in the early epoch of galaxy formation. In particular, the first generation of stars — commonly called 'Population III'— which formed from primordial, essentially metal-free matter, should provide the oldest bright objects in galaxies. Therefore, the identification and the analysis of the properties of this class of stars should offer an unique tool for investigating the chemical and physical conditions in the very early history of our universe.

Owing to their importance for several fundamental cosmological questions, several attempts have already been made to find zero-metal and/or extremely metal-poor stars. The first extensive search for Pop. III stars has been performed early by Bond (1980), who discovered only a few stars with metallicity [Fe/H] $= -3$ (i.e. a iron content of only 1/1000 of the solar value); more recently the sample of extremely metal-poor stars has significantly been increased, mainly due to extensive Wide-Field Objective-Prism Surveys, and especially due to the Preston-Shectman survey (Beers, Preston, & Shectman 1992, usually also called HK survey). Although none of these stars shows a 'true' Pop. III chemical composition, there is an increasing number of stars with metallicity [Fe/H] < -3, for which accurate post-detection analysis can be performed. In addition, one can expect that forthcoming high resolution spectroscopy from the new generation of 10 m-class telescopes will lead to a big improvement in the search for this class of peculiar objects. Undoubtedly, unprecedented results in this field will be achieved with planned space-based survey instruments such as GAIA.

In order to fully understand the results of these surveys, it is necessary to investigate theoretically not only the main evolutionary properties of low-mass metal-free stars, but also the changes of the surface chemical composition appearing during that evolution. These may be caused by accretion of metal-rich matter from the interstellar medium and/or by internal mixing of matter processed by nuclear reactions. One significant observational evidence, which has yet to be explained, is that the number of carbon-enhanced stars increases considerably when decreasing the metallicity below [Fe/H] ≈ -2.5 (Rossi, Beers, & Sneden 1999). Several of the extremely metal-deficient carbon stars show a large carbon abundance as well as nitrogen enrichment ([C/Fe] resp. [N/Fe] $\gtrsim$ 2). In some of these carbon-enriched stars the abundances of $s-$process elements are enhanced, too (see Hill et al. 2000 and reference therein). This obviously implies that in extremely metal-poor stars mechanisms are at work which increase the probability for producing carbon-rich objects.

In the last decades, several theoretical studies of the structural and evolutionary properties of extremely metal-poor and metal-free stars (see for instance the reviews by Castellani 2000 and Chiosi 2000 and references therein) have shown how the lack of heavy elements — mainly of CNO-cycle catalysts — produces evolutionary features, which are rather peculiar in comparison to stars of finite initial metallicity. One of these properties – investigated by Fujimoto and coworkers (Fujimoto, Iben, & Hollowell 1990; Hollowell, Iben, & Fujimoto 1990; Fujimoto, Ikeda, & Iben 2000) – is the evolution during the He-flash. Like their more metal-rich counterparts, metal-free stars with a mass of about 1.0 $M_{\odot}$ reach the conditions necessary for igniting triple-alpha reactions inside the He core at the tip of the red giant branch(RGB). The electron degeneracy of the surrounding material leads to a runaway of the He burning, the He core flash. The quoted authors discovered that the small entropy barrier between hydrogen- and helium-rich material in Pop. III stars allows the convective zone, which is produced by the huge energy release of He burning, to penetrate the overlying hydrogen-rich layers. The resulting inward migration of protons into high-temperature regions (referred to as 'He-Flash Mixing', hereinafter HEFM) leads to a H shell flash. As a consequence, when the convective envelope is deepening and merging with the H-flash driven convective zone (HCZ) later on, the surface is enriched with a large amount of matter that has experienced He-burning reactions and furthermore has been processed in H fusion during the H-flash. Thus, the chemical composition of the initially metal-free stellar surface is strongly altered and in particular carbon-enriched. These results provide an attractive working hypothesis for explaining the peculiar chemical patterns observed in extremely

metal-deficient stars.

In a previous paper (Weiss et al. 2000, hereinafter Paper I), we have investigated the evolutionary properties of low-mass metal-free objects from the Zero Age Main Sequence (ZAMS) to the He-flash at the tip of the RGB, using updated physical inputs and, for the first time, accounting also for atomic diffusion. In view of the peculiar structural properties which characterize Pop. III stars (see Cassisi & Castellani 1993, Paper I), special care was taken to use an appropriate and complete nuclear reaction network. Furthermore, numerical experiments were performed with the aim of testing how the evolution of a metal-free star is affected when its surface is polluted by metal-rich matter through encounters with interstellar gas clouds — a scenario suggested in order to explain the absence of truly zero-metal stars and the relative paucity of extremely metal-poor objects (Yoshii 1981). We found that the metals in the accreted matter fail to reach the nuclear-burning regions, so that the main structural and evolutionary properties of the stars are not affected by the external pollution; it was also clearly shown that it is quite difficult to discriminate observationally between a polluted Pop. III star and a very metal-poor Pop. II object in this phase of evolution.

In Paper I we stopped the computations soon after the onset of the He-flash and did not investigate the evolution during the further development of the He flash at the RGB tip. This had been done by, e.g., Fujimoto et al. (1990), but until now these results have not been supported by independent investigations[6]. In the present work we present a reanalysis of the evolution during the He-flash phase, covering a larger parameter space with respect to the work by Fujimoto and coworkers.

The main characteristics of the evolutionary code used in the present investigation are discussed in the next section; special emphasis is laid upon the numerical algorithms adopted to follow the evolution during the He-flash, and the most relevant differences with respect to previous investigations are indicated. In § 3 the evolution through the He core flash in some selected models is presented together with a discussion of the dependence of the subsequent evolution on the 'initial conditions', like stellar mass and chemical composition. In the same section, we discuss the change in the surface chemical abundances caused by the appearance of a H shell flash like the one investigated by Fujimoto et al. (1990). In § 4 we extend the computations for some selected models, which experience a H shell flash, to the following evolutionary phases; we discuss the evolution all along the He-core and -shell burning phase, and compare our results with those corresponding to He-burning models in case that no H shell flash in the HEFM had occurred. A first comparison with observed extremely metal-poor objects is made in § 5. Conclusions and a brief discussion close the paper.

[6] In a different context, results similar to the one discussed by Iben and coworkers has been obtained by Cassisi, Castellani, & Tornambé (1996); here the He shell flash in an $0.8\,M_{\odot}$ model during the thermal-pulse phase on the Asymptotic Giant Branch was discussed.

2. The stellar evolution code.

All calculations reported about in this paper were done with the Garching stellar evolution code (Weiss & Schlattl 2000), which is based on the original program developed by Kippenhahn, Weigert, & Hofmeister (1967). The program in its present version is capable of calculating precise solar models (Schlattl 2000; Schlattl & Weiss 1999) as well as following the evolution of low-mass stars into the latest phases of their evolution (Wagenhuber 1996; Schlattl & Weiss 1999).

2.1. Numerical details.

The evolution through the He-flash can be followed in an acceptable amount of computing time thanks to the grid routine implemented by Wagenhuber & Weiss (1994), which ensures a sufficiently high accuracy in the linearization of the stellar structure equations. Moreover, the algorithm to determine the under-correction factor, i.e. the actually applied fraction of the correction found in each iteration step, has been improved considerably. By further limiting the time-step with a constraint on the change of the He-burning luminosity ($L_{\rm He}$), the critical phase of the He-flash ($\log(L_{\rm He}/L_{\odot}) > 7$) can be followed with about 200 models, and with at most about 200 iterations per model around the maximum He luminosity ($\log(L_{\rm He}/L_{\odot}) \approx 10$).

The helium flash induced mixing found by Fu-

jimoto et al. (2000) results in a qualitative agreement with the observed surface chemical patterns of stars in the HK survey; however, their theoretical investigation has been performed by using a limited reaction network and a crude procedure to follow the fast mixing process during the HEFM episode. On the other hand the development and the general properties of the HEFM phenomenon strongly depend on where, inside the structure, the ingested hydrogen is burnt. Fujimoto et al. (2000) assumed that the hydrogen engulfed by the convective zone is mixed instantaneously down to a position at which the lifetime of a proton against capture in the $^{12}C(p,\gamma)^{13}N$ reaction is equal to the timescale of convective mixing. We wish to remark that in a previous paper, Hollowell et al. (1990) stated that they adopted a time-dependent mixing scheme which treats convection as a random-walk processes with the rate of convective cell diffusion being a function of the local mixing length and of the local buoyancy velocity. It is not clear to us whether Fujimoto et al. (2000) still use this approach, or whether they assume instantaneous mixing.

In order to determine how deeply hydrogen is mixed during the HEFM into the helium flash driven convective zone (HECZ), it is crucial to treat the mixing as a time-dependent process and to consider carefully the simultaneous mixing and burning processes. In the present investigation, we therefore improved the treatment of mixing and burning in our program. The equations for microscopic diffusion, convection (see below) and nuclear burning are solved in one common scheme (Schlattl 1999); this also implies that the hydrogen and helium networks are solved simultaneously. This is necessary for the correct treatment of the nuclear evolution during those phases, when H and He burning are operating at the same time, as is the case in the core of evolved low-mass main sequence-stars ("CNO-flash", Weiss et al. 2000; Fujimoto et al. 1990) of Pop. III and during the HEFM.

In our approach convection is treated as a fast diffusive process where the diffusion constant is proportional to the convective velocity obtained from a convection theory (Langer, El Eid, & Fricke 1985). When the HECZ touches the H-rich layers at the lower boundary of the H-burning shell, the ingested hydrogen interacts with ^{12}C to produce ^{14}N (CNO I), releasing a huge amount of energy ($\log(L_H/L_\odot) \gtrsim 6$). The movement of the outer boundary of the convective zone is not smooth, but proceeds discontinuously and therefore this phase is difficult to follow numerically. Even if the number of grid points is increased considerably, the step-wise motion could not be suppressed totally. Consequently it is very difficult to determine in advance when the next H-rich shell is mixed into the hotter regions and the appropriate next time-step is nearly impossible to determine. Using time-steps too large shortly before the onset of mixing, the violent H-burning phase may be missed, while time-steps too short make the computation of the whole phase very time consuming.

The reason for this behaviour is that the stellar evolution program calculates the physical structure of a model at a certain epoch and afterwards uses this structure (in particular the density- and temperature-profile) to calculate the chemical evolution during a certain time interval following. The solution of all the stellar structure equations (physical as well as chemical variables) in a common scheme would be possible, but it is not advisable, since during this phase already a large number of iterations ($\gtrsim 40$) are needed for the physical variables alone. Including the chemical evolution in the solution of the stellar structure would increase the computing time by a factor of three[7].

The separation of the chemical and structural part, dictated by computational efficiency, however has the consequence that, during the solution of the physical structure, any additional mixing which is related to the movement of the boundary of the convective zone is not taken into account. Hence, when the upper boundary of the HECZ moves outward, the program treats hydrogen burning for the current position only, yielding smaller energies than when additional hydrogen is mixed down into hotter regions from layers just becoming convectively unstable.

If the time step during this phase is chosen too large, all protons will be captured completely in the computation of the chemical evolution. The energy released, however, will be that of the total (and larger) time step. The specific energy release per second is therefore lower than it actually would

[7] 4 physical variables (L, P, T, r) plus 9 chemical species (^1H, ^3He, ^4He, ^{12}C, ^{13}C, ^{14}N, ^{15}N, ^{16}O, ^{17}O)

be if the additional mixing due to the advance of the convective boundary had been included. With very short time-steps one could better follow the movement of the convective zone and thus changes in the hydrogen luminosity. However, experience shows that the (numerically) still discontinuous penetration of the HECZ into H-rich layers leads to oscillations in the hydrogen luminosities, and the resolution of these would demand a disproportionately high number of time steps.

Whenever the He-flash driven convective zone penetrates into a region of non-vanishing hydrogen abundance, additional energy is released on a short time scale. As long as the hydrogen abundance is smaller than approximately 0.05, the additional energy from the violent hydrogen fusion is negligible, because of the fact that the helium luminosity is the dominant energy source. When the HECZ is advancing to regions with hydrogen abundances higher than about 0.05, the large H abundance in this zone causes a significant increase of the H-burning rate, which drives a further expansion of the convective zone (see Fig. 4). The numerical code then has to follow the ensuing H-burning runaway ($\log(L_{\rm H}/L_\odot) \gtrsim 10$), during which the subsequent expansion of the star may even lead to a cessation of helium burning.

We found that the most appropriate quantity to determine the onset of the H-flash is

$$\delta L = \langle L_{\rm nuc}(\Delta t)\rangle / L_{\rm nuc}(t_0), \qquad (1)$$

where $L_{\rm nuc}(t_0)$ is the nuclear luminosity as calculated in the solution of the stellar structure equations, and $\langle L_{\rm nuc}(\Delta t)\rangle$ is the average nuclear luminosity derived from the chemical changes within $\Delta t = t_1 - t_0$. This quantity effectively controls the consistency between the instantaneous energy generation and the subsequent chemical evolution based on it. Whenever $|1 - \delta L|$ exceeds a certain limit (presently set to about 0.7), the chosen time-step is immediately reduced and the chemical evolution is recalculated. The time-step is decreased until $|1 - \delta L|$ becomes sufficiently small. With this and additional criteria for the determination of time steps and grid resolution, it is possible to follow numerically the He-flash and HEFM evolution of low-mass metal-free stars both accurately and efficiently.

In the lower panel of Fig. 1 δL during the approach of the HECZ to the H-rich layers is shown. Already at $t - t_0 \approx 10\,$yr, i.e. before $L_{\rm H}$ exceeds $L_{\rm He}$, hydrogen is mixed into the He-burning convective zone, causing an increase in $\log(L_{\rm H}/L_\odot)$ from initially about -0.5 to 2.5 (thick solid line in upper panel of Fig. 1). This energy release is, however, negligible compared to the energy produced by the fusion of helium. Hence, even with relatively large time-steps, $|1 - \delta L|$ remains below 0.5. When the amount of ingested hydrogen is sufficient to affect the subsequent evolution ($t - t_0 \approx 29\,$yr), δL becomes larger than 2, leading to a drastic decrease of the time-step. The subsequent evolution of $L_{\rm H}$ and $L_{\rm He}$ is resolved accurately ($|1 - \delta L| < 0.5$).

2.2. Input physics.

In order to describe the chemical evolution of the star we follow the abundances of H, ^{3}He, ^{4}He, ^{12}C, ^{13}C, ^{14}N, ^{15}N, ^{16}O, ^{17}O, without assuming *a priori* equilibrium compositions for these chemical elements.

Since the metal distribution in our models can show strong deviations with respect to the usually adopted scaled-solar mixture, we decided not to use the most updated equation of state (like OPAL-EOS; Rogers, Swenson, & Iglesias 1996), but the Saha-equation for the outer stellar layers, and a simplified equation of state for a degenerate electron gas in the core regions (Kippenhahn & Weigert 1990)[8]. The switching point between these two equations of state is determined by the position where either carbon or helium (in case there is no carbon present) is fully or maximally ionized.

For the radiative opacity we have used, unless stated differently (see below), the tables provided by Iglesias & Rogers (1996) for temperatures above $T > 10000$ K, and for low temperatures ($T < 8000$ K) those by Alexander & Fergusson (1994). In the intermediate temperature range a smooth transition between the two tables is used. Both opacity table sets were computed by using a scaled-solar mixture for the heavy-element distribution. For electron conduction opacities we used a program employing the results by Itoh et al. (1983), which allows the calculation of the opacity for arbitrary abundances of the most important

[8]The dependence of the results on this choice will be discussed in the next section.

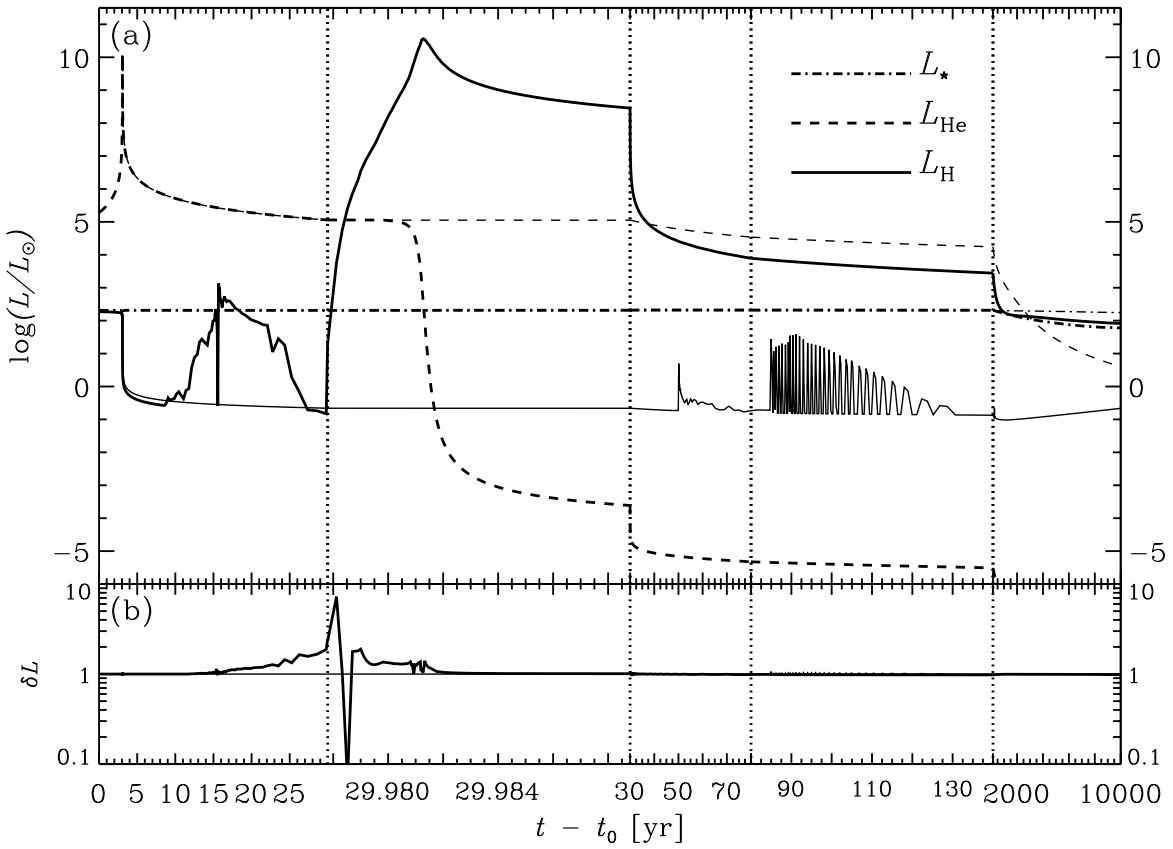

Fig. 1.— (a) The evolution of the total, the H-burning, and the He-burning luminosities during the major He core flash in our standard model experiencing the H-flash (thick lines, $t_0 = 6.9\,$Gyr), and in the model without H-flash (thin lines, $t_0 = 6.5\,$Gyr). (b) δL (Eq. 1), the ratio between the mean nuclear energy release during each time-step and the initial one. This quantity is used to detect the onset of the H-flash in the computations (see text for more details). Note the changes in the x-axis scale which are delimited by the vertical dotted lines.

elements.

The diffusion constants for the gravitational settling of heavy elements are calculated by a routine provided by Thoul (private communication), which solves Burgers' equation for a multicomponent fluid (Thoul, Bahcall, & Loeb 1994). For the treatment of convection we apply the mixing-length theory (Vitense 1953) with the parameter α=1.6. The energy losses from photo-, pair- and plasma-neutrinos are calculated according to Munakata, Kohyama, & Itoh (1985). Mass loss has been accounted for by using the Reimers' formula (Reimers 1975) with η=0.4.

3. The helium flash induced mixing.

The evolutionary and structural properties of low-mass, metal-deficient stars have been described at several instances (see for instance Cassisi & Castellani 1993 and Paper I) and will not be repeated here. We wish to focus our attention on the development of the He-flash induced mixing episode and, primarily, on its dependence on stellar parameters such as the initial helium abundance. The occurrence and the details of the HEFM phenomena have been discussed in detail by Hollowell et al. (1990). Here we emphasize the differences between their results and ours.

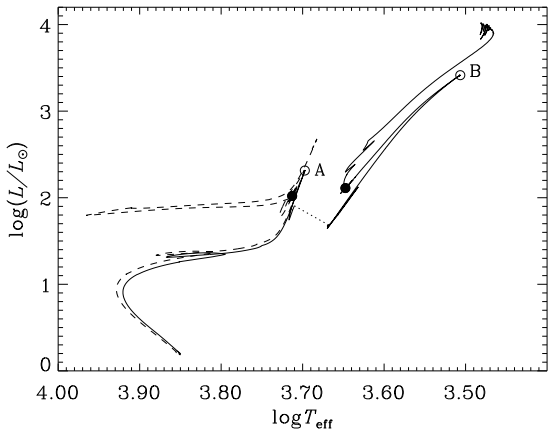

Fig. 2.— The evolution in the H-R diagram of a $1\,M_\odot$ star with initial helium abundance $Y_i = 0.23$ (solid line) and $Z = 0$ from the ZAMS up to the helium shell-burning phase. The open circles labelled by A and B correspond to the onset of the first (major) and the second He-flash, respectively. The fast transition from A to a phase of slow shell burning is indicated by the dotted segment. Also shown, for comparison, is the track of the same model, but with an initial helium abundance of 0.24 (model S3), which does not experience a hydrogen flash. The filled circles indicate the beginning of the central He-burning phase.

3.1. The hydrogen flash.

Our 'standard' model is a metal-free one with mass equal to $1\,M_\odot$ and an initial helium abundance $Y_i = 0.23$, computed by neglecting both atomic diffusion and possible external pollution. The main properties of this model are listed in the first line of Table 1. In this table we report initial conditions, main assumptions which characterize each case, the information whether the HEFM leads to a H-flash, and the final relevant surface abundances at the end of the H resp. He-flash for all the experiments performed (§ 3.2). The evolution of our standard model in the H-R diagram is shown in Fig. 2.

The major He core flash occurs when the surface luminosity is equal to $\log(L/L_\odot) = 2.314$, i.e. a factor of ≈ 1.5 lower than the value attained by the model of Iben and coworkers. At this stage, the mass of the He core is $M_{\rm cHe} = 0.482\,M_\odot$. The mass shell of maximum energy release by He burning, $M(\epsilon^{\rm He}_{\rm max})$, is located at $M_r = 0.151\,M_\odot$. These values are in fair agreement with the ones obtained by Cassisi & Castellani (1993). The evolution of $M_{\rm cHe}$ and $M(\epsilon^{\rm He}_{\rm max})$ is shown in Fig. 3.

Significantly different results were found by Fujimoto et al. (1990). In their model (of same mass) the size of the H-exhausted core at He-flash ignition is $0.528\,M_\odot$ and $M(\epsilon^{\rm He}_{\rm max})$ is $0.41\,M_\odot$. We do not know the reason for such a large difference in the location of the He-flash ignition, but we suspect it could be due to the choice of radiative and/or conductive opacities adopted by Fujimoto et al. (1990), or differences in the treatment of plasma-neutrino emission. It should be emphasized that the value of $M(\epsilon^{\rm He}_{\rm max})$ is very important for the occurrence of a H-flash. The closer $M(\epsilon^{\rm He}_{\rm max})$ is to the border of the He core, the higher is the probability for the HECZ to reach the H-rich layer.

Soon after the He-flash sets in a convective shell

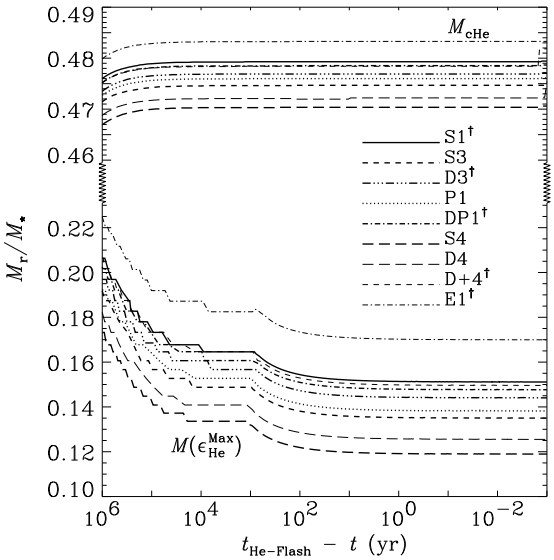

Fig. 3.— The evolution of the He core mass ($M_{\rm cHe}$) and of the mass shell where the He-burning energy release is at maximum [$M(\epsilon^{\rm He}_{\rm max})$] for different model sequences. The notation of the models follows Table 1, where the input physics of the various sequences is defined. The solid line corresponds to our standard model. The symbol † is used to identify the models experiencing the H-flash.

TABLE 1

MAIN PROPERTIES OF VARIOUS NUMERICAL EXPERIMENTS.

			Physics					Properties[a]				
Mod.[b]	Y_i	$\frac{M_\star}{M_\odot}$	$\frac{D_C}{D_{\rm MLT}}$[c]	$\frac{D_{\rm mic}}{D_{\rm Th}}$[d]	Poll.[e]	EOS	κ[f]	$L_{\rm He}^{\rm max}$[g]	Y^S[h]	$X_{\rm C}^S$	$X_{\rm N}^S$	$\frac{X^S(Fe)}{X_i^S(Fe)}$
S1†	0.23	1.0	1	—	no	Saha	solar	10.11	0.477	0.0088	0.0043	···
S2†	0.235	1.0	1	—	no	Saha	solar	10.06	0.478	0.0085	0.0040	···
S3	0.24	1.0	1	—	no	Saha	solar	10.02	0.241	0.0	0.0	···
S4	0.25	1.0	1	—	no	Saha	solar	9.92	0.251	0.0	0.0	···
C1†	0.23	1.0	$1^{\rm CM}$	—	no	Saha	solar	10.10	0.472	0.0086	0.0041	···
O1†	0.23	1.0	1	—	no	Saha	C&N	10.10	0.466	0.0088	0.0035	···
E1†	0.23	1.0	1	—	no	OPAL	solar	10.54	0.436	0.0080	0.0032	···
A1†	0.23	1.0	0.01	—	no	Saha	solar	10.10	0.399	0.0060	0.0026	···
A3	0.24	1.0	10^3	—	no	Saha	solar	10.02	0.241	0.0	0.0	···
D1†	0.23	1.0	1	1.0	no	Saha	solar	10.13	0.469	0.0064	0.0069	···
D3†	0.24	1.0	1	1.0	no	Saha	solar	10.05	0.471	0.0066	0.0066	···
D4	0.25	1.0	1	1.0	no	Saha	solar	9.96	0.240	0.0	0.0	···
D+4†	0.25	1.0	1	5.0	no	Saha	solar	10.09	0.459	0.0092	0.0035	···
P1	0.23	1.0	1	1.0	yes	Saha	solar	10.04	0.232	1.4×10^{-4}	3.4×10^{-5}	0.032
P3	0.24	1.0	1	1.0	yes	Saha	solar	9.96	0.241	1.4×10^{-4}	3.4×10^{-5}	0.032
DP1†	0.23	1.0	1	1.0	yes	Saha	solar	10.09	0.464	0.0086	0.0040	0.013
DP3	0.24	1.0	1	1.0	yes	Saha	solar	10.0	0.230	1.4×10^{-4}	3.5×10^{-5}	0.032
M1†	0.23	0.82	1	—	no	Saha	solar	10.30	0.512	0.0069	0.0098	···
M3†	0.24	0.81	1	—	no	Saha	solar	10.25	0.550	0.0086	0.0097	···
B1†	0.23	0.82	1	1.0	yes[i]	Saha	C&N	10.34	0.520	0.0123	0.0050	3.4×10^{-4}
B2†[j]	0.23	0.82	1	1.0	yes[i]	Saha	C&N	10.31	0.502	0.0115	0.0048	3.9×10^{-4}

[a] Abundances after dredge-up (H-flash) resp. at beginning of HB

[b] Models experiencing a H-flash are denoted by †.

[c] Ratio of actual diffusion constant to the one derived from mixing length theory (Vitense 1953, $\alpha_{\rm MLT} = 1.6$). "CM" marks model calculated with the theory of Canuto & Mazzitelli (1991, 1992, $\alpha_{\rm CM} = 0.8$).

[d] Ratio of actually applied microscopic diffusion constant to the values derived by Thoul et al. (1994).

[e] $Z = 0.02$, $\Delta M = 0.01\, M_\odot$ (mass of additional, polluted matter)

[f] Heavy element distribution used in the opacities: 'solar' and 'C&N' mean that a scaled-solar resp. carbon- and nitrogen-enhanced mixture has been adopted.

[g] Logarithm of the maximum He-burning luminosity in units of the solar luminosity.

[h] S=surface, i=initial

[i] In this sequence, the value of $\Delta M = 3 \times 10^{-4}\, M_\odot$ has been chosen in order to match the observed [Fe/H] value in the star CS22892-052 (see text for more details).

[j] No mass-loss in this model, i.e. $\eta_{\rm Reimers} = 0$

appears, like in the model computed by Fujimoto et al. (1990). However, in our computation this convective zone reaches H-rich matter $\approx 10\,\mathrm{yr}$ after the He core flash, whereas in the work by Fujimoto et al. (1990) the HEFM occurs immediately after the He-flash ($\approx 10^{-3}\,\mathrm{yr}$). This difference is due to the much smaller distance between $M(\epsilon^{\mathrm{He}}_{\mathrm{max}})$ and the outer edge of the H-exhausted region in Fujimoto et al.'s (1990) model compared to our computations.

Fig. 1 shows the evolution of the energy release produced by H and He burning during the major He core flash for two models: the standard one and a model which does not experience a H-flash (models S1 & S3, see also Fig. 2). At the onset of the H-flash, i.e. when the H-burning luminosity exceeds that of He-burning, the outer border of the convective shell has reached a mass shell with $X = 0.055$. This value has to be compared with the value of 0.023 listed by Fujimoto et al. (2000), which actually belongs to an $0.8\,M_{\odot}$ model, but which can be extrapolated safely to one with $M = 1\,M_{\odot}$.

As soon as H is carried into the interior, it starts to be burnt at an extremely high-rate due to the high temperatures in these regions, and this deeply affects the following evolution of the star. This behaviour is as in the computations by Fujimoto and coworkers. We note that in this model experiencing a H-flash the amount of H ingested during the HEFM phase is $6.5 \times 10^{-4}\,M_{\odot}$.

The evolution of the convective zones during the major He core flash is shown in Fig. 4. The single HECZ separates into two zones soon after the ingestion of H, because two burning shells are developing (an exhaustive description of this process can be found in Hollowell et al. 1990).

This behaviour is in agreement with the computations performed by Hollowell et al. (1990), although the treatment of the driving mechanism, the CNO-burning, is different: Hollowell and coworkers assumed that the abundances of isotopes involved in the CNO-cycle are locally in equilibrium, and that all of the energy from the CN-chain is released whenever a proton is captured on ^{12}C, whereas we adopt a more accurate treatment for the H-burning network (see § 2.1). In passing, we note that our models support the suggestion by Hollowell et al. (1990), according to which a more realistic treatment of the H burning should have the only effect of producing a wider H-burning shell.

However, at odds with the results obtained by Hollowell et al. (1990), in our computations of the HEFM the He-burning luminosity attains negligible values, and the structure is fully supported by the H-burning shell. Besides, due to the H-flash the size of the He core is significantly reduced in comparison with the value reached just before the He-flash.

About 100,000 years after the HEFM, the convective envelope deepens and merges with the convective zone located above the H-burning shell (the 'HCZ'), the lower boundary of which has, as also shown by Hollowell et al. (1990), moved outward. At the end of this process, a huge amount of matter processed by both H and He burning is carried to the surface of the star, polluting its initially metal free chemical composition. Thus, the stellar surface is strongly enriched by helium ($Y_{\mathrm{surf}} \approx 0.5$) and the global metallicity is equal to $Z = 0.0131$. However, unlike a Pop. I star, the most abundant heavy elements at the stellar surface are the various isotopes of carbon and ni-

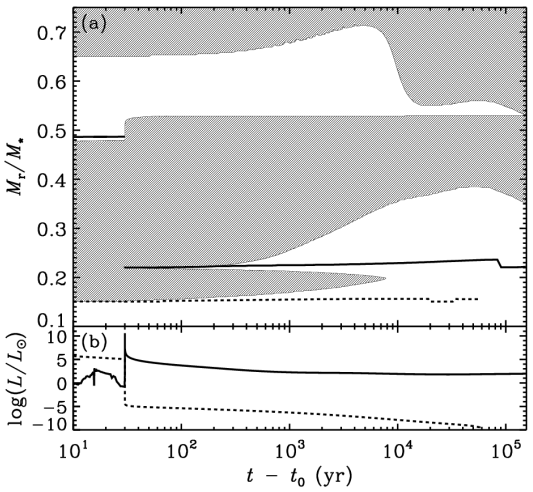

Fig. 4.— (a) The development of the different convective zones – indicated by shaded areas – as a function of time in our standard model. The solid and dashed lines represent the mass shells of maximum energy release by H- resp. He-burning. (b) The evolution of L_{H} (solid) and L_{He} (dashed line) of the same model.

trogen. The surface abundances of both elements are listed in Table 1. It is evident that the He-flash induced H-flash, if operating in real Pop. III stars, produces very significant changes in the chemical composition of the star, preventing its identification as a 'true' metal-free star.

As a result of the dredge-up of metal-rich matter, the low-temperature opacity is increased drastically. This produces an abrupt jump in the effective temperature visible in the HR-diagram (Fig. 2; indicated by the dotted part of the track).

The ceasing fusion of He after the H-flash yields a new-born shell H-burning object, climbing up its own RGB. However, this time the H-burning shell is moving through a helium-rich region and the energy production rate is quite large in comparison with the previous evolution. About 50 million years after the first He-flash, when the He core mass is equal to $0.452\,M_\odot$, a second He-flash develops at $M_r = 0.027\,M_\odot$. The smaller He core mass and the – compared to the first flash – lower $M(\epsilon^{\rm He}_{\rm max})$ can both be explained by a substantial decrease of the central electron degeneracy during the previous He ignition. This argument is supported by the strength of the second He-flash, which is significantly weaker than that of the first one.

In the subsequent evolution no further mixing episode between the He-burning region and the outer envelope was found. The core He burning and later phases will be described in § 4. In the next section we concentrate on the initial and physical conditions, which might influence the development of the H-flash.

3.2. The dependence of the H-flash on the initial conditions.

The results discussed in the previous section have clearly shown that, at least for the "standard" model, our computations provide independent support for the results found earlier by Hollowell et al. (1990) and by Fujimoto et al. (2000). Nevertheless, there is the important difference between both investigations concerning the location where the first He-flash starts. As already stated in the previous section, $M(\epsilon^{\rm He}_{\rm max})$ is closer to the border of the H-exhausted region in the models provided by Fujimoto and coworkers than in ours.

Since the position of maximum He-burning energy release is crucial in defining whether the HEFM and the follow-up H-flash occur, we wish to investigate if and to what extent the value of $M(\epsilon^{\rm He}_{\rm max})$ depends on the initial conditions and on the treatment of various physical processes. Therefore, different models have been evolved through the major core He-flash. In detail, we have accounted for changes in the initial helium abundance, the stellar mass, the amount of external pollution, the efficiency of atomic diffusion, and the uncertainty in the mixing length theory, which is used for determining the velocity of the convective cells in the adopted time-dependent scheme. Furthermore, two different sets of equations of state and opacities have been applied. In Table 1, the main properties of these models are listed. The models which experience a H-flash are identified by †.

From the data listed in this table, one notices that the evolution through the HEFM phase strongly depends on the initial conditions. For instance, increasing the initial He abundance from 0.23 to 0.24 inhibits the H-flash. The inward shift of $M(\epsilon^{\rm He}_{\rm max})$ is only partially compensated by a decrease of the He core mass (Fig. 3), disfavouring a H-flash (see also Fig. 1).

We have computed some sequences accounting also for atomic diffusion as described by Thoul et al. (1994) (models 'D'). These models reveal that microscopic diffusion increases the probability for a H-flash (compare models S3 and D3). Interestingly, by artificially increasing the diffusion coefficients by a factor of 5, the internal structure of model D4, which would not experience a H-flash, is modified in such a way that a H-flash does occur (model D+4).

Since the strength of the H burning, and probably also the appearance of a H-flash, strongly depends on where inside the HECZ the ingested protons are burnt — the deeper the burning occurs, the higher the burning rate — we computed models with different convective velocities and convective "theories". In our standard model the velocity of the convective cells are obtained from the mixing length theory (Vitense 1953, MLT). We have computed a model again, which usually experiences a H-flash, but decreasing the MLT velocity by two orders of magnitude (model A1). This model still shows a H-flash. In the same manner, increasing the MLT velocity by two orders of mag-

nitude in model S3, where no H-flash occurs, does neither lead to the development of a H-burning runaway (model A3). The convective velocity itself, therefore, is of no influence on the flash.

Furthermore, we have verified that our results do not depend on the convection theory applied. For this purpose, one sequence (C1) has been computed using the convection theory by Canuto-Mazzitelli (Canuto & Mazzitelli 1991, 1992, CM). Again, a H-flash occurred during the HEFM phase as in A1. Since the results are stable against changes in the convection theory and against large variations of the convective velocities, we consider them to be reliable, despite the unavoidable approximations one has to make when including time-dependent mixing in convective zones.

In view of the results discussed in Paper I, we have also checked whether external pollution can affect the occurrence of a H-flash. Therefore, we computed additional models (P1 & P3) by artificially changing the chemical composition in the outer $0.01\,M_{\odot}$ of the star, making it similar to the solar one (see Paper I for more details). We found that external pollution disfavours the development of a H-flash (see Table 1 and Fig. 3).

All numerical experiments discussed so far have been performed by using opacities where the metals are in scaled-solar proportions. As described in § 3.1, after the H-flash the "metals" in the convective zone above the H-burning shell (HCZ) consist almost entirely of carbon and nitrogen; therefore the boundaries of the HCZ should be determined more accurately with opacity tables that have a more realistic heavy element distribution. It is important to notice that the position of the lower boundary of the HCZ crucially determines the amount of metals which are later dredged-up to the surface.

We performed some additional experiments by using opacity tables taking into account the C- and N-enhancement characteristic for these models. For this purpose we computed opacity tables for the high-temperature regime, considering various He abundances but including only C and N in the heavy element distribution[9]. In detail, we assumed that the C and N fractional abundances are both equal to 0.5 by mass within the metal group. For lower temperatures the Alexander & Fergusson (1994) tables are used, which were only available for a weak carbon- and nitrogen-enhancement (3×solar, private communication). Since the opacity evaluations in the very outer regions are less crucial for the later mixing process, we think that these tables are sufficiently accurate for the present investigations.

We ran model O1 with these new opacity tables and examined, in particular, if the boundaries of the different convective zones change with respect to the models with scaled-solar opacities. No significant differences in the internal properties of the structure and the final surface chemical composition could be detected.

A further test of the dependence of our results on the adopted physical input consisted in computing a model (E1) using the most accurate EOS presently available: the OPAL EOS (Rogers et al. 1996). Since this equation of state does not extend to the temperatures of He burning, it was extended by the simpler EOS described in section 2.2. The OPAL EOS is available for three metallicities ($Z = 0.0, 0.2, 0.4$); as for the "standard" opacity tables, metals are assumed to be scaled solar. We included this equation of state by interpolating between the available tables at each stellar layer to take into account the large variation of metal content in the star. As a result, a stronger He-flash occurred in model E1 than in the standard case S1, further increasing the probability of a H-flash during the HEFM.

In order to test the effect of mass loss, we changed the mass loss rate (model B1 & B2). No effect on the general behaviour of the HEFM process was found. This is explained by recalling that the outer envelope properties of RGB stars do not have much influence on the internal properties.

As a general rule, summarizing the results shown in Fig. 3 and listed in Table 1, *all those changes in the initial conditions and/or in the physical input, which can contribute to an increase of the electron degeneracy, and thus cause the location of He ignition to move closer to the border of the He core, favour the occurrence of a H-flash.* This has the additional effect that less energy released in the He-flash needs to be used for expanding overlying layers. This statement is further sup-

[9] These opacity tables have been computed by using the tool available at http://www-phys.llnl.gov/Research/OPAL/index.html, provided by the Livermore Laboratory Opacity Group.

ported by the observation that the occurrence of a H-flash in stars with smaller masses is less dependent on the initial conditions and physical processes included. These stars intrinsically have a more strongly degenerate electron gas in the center and thus the development of a H-flash in these stars is less sensitive to the various input parameters we investigated above. As an example, we calculated model M1 and M3 with $0.82\,M_\odot$, which both have a larger maximum He-energy production ($L_{\rm He}^{\rm max}$) in the He flash than almost all $1\,M_\odot$ models and which both undergo a H flash (see Table 1).

An important result of the experiments presented is that the final surface abundances of C and N in all models experiencing a H-flash during the HEFM stage are quite similar (they differ at most by a factor of 2, cf. Table 1). This means that despite the difficulties in the numerical treatment of the HEFM and the H-flash phases, the computations provide quite robust results for the relevant surface chemical abundances, which will be compared to observations in § 5.

4. The post He-flash evolution.

4.1. The core He-burning evolution.

Irrespective of whether a H-flash occurs or not, as soon as the model attains the thermal conditions necessary for the quiescent burning of He via the triple-alpha reaction, it displays the configuration typical of a Horizontal-Branch (HB) star.

Until now only one theoretical investigation (Cassisi et al. 1996) has addressed the problem of the evolution of low-mass metal-deficient stars during the He-burning phases. However, in that work the occurrence of HEFM was neglected and the post He-flash evolution was investigated without taking into account the changes in the stellar properties induced by this process.

In this section we analyze the evolution of a model which has experienced a H-flash during the HEFM. We consider a $1\,M_\odot$ model (S1) — the same one which we have defined as our standard model in the previous discussions — and the $0.82\,M_\odot$ models B1 & B2. The latter models have been chosen because their age ($\approx$ 13 Gyr) at the Main Sequence Turn Off could be that of a contemporary Pop. III star.

The evolution in the H-R diagram of the $1\,M_\odot$ model experiencing the HEFM is shown in Fig. 2 (model S1). For comparison, the track during the same evolutionary phase for model S3 (no H-flash) is plotted (dashed line); filled circles indicate the location of the Zero Age Horizontal Branch (ZAHB) for both models. We notice that despite the quite different evolution during the previous core He-flash, no major difference in the ZAHB luminosity ($\Delta \log(L/L_\odot) \approx 0.1$) exists. The ZAHB effective temperature is changed only little, too ($\Delta \log T_{\rm e} \approx 0.06$). The reasons why the ZAHB location of the model experiencing a H-flash is slightly brighter and cooler have been identified to be the larger He envelope abundance and the larger surface metallicity, respectively. We also mention that the value of the effective temperature for the star undergoing HEFM is probably not precisely determined by our models, since the metal mixture of the low temperature opacities does not exactly match the one at the stellar surface.

The time spent in core He burning is 77 Myr for the "standard" model S1 and 51 Myr for model S3 without HEFM. This difference is due to both the smaller He core at the beginning of the central He-burning phase and the larger efficiency of the H-burning shell in the model experiencing a H flash.

Interestingly, the evolutionary track in the H-R diagram of model S3, which does not experience the H-flash, is quite similar to the results by Cassisi et al. (1996). However, the core He burning lifetime in their models is longer by a factor of ≈ 2. This is mainly due to neglecting semiconvection during the quiescent He burning in our computations. Ignoring this effect probably also caused the occurrence of a blue loop which is not present in Cassisi et al.'s (1996) work.

The evolution of the $0.82\,M_\odot$ model in the H-R diagram is shown in Fig. 5. In order to test the effect of mass-loss on the overall evolution, the sequence has been computed twice, first without mass-loss (model B2 in Table 1) and then using a Reimers' mass-loss law with $\eta_{\rm Reimers} = 0.4$ (model B1). Due to the high mass loss in model B1 the mass of the star has been reduced to $0.63\,M_\odot$ at the beginning of the HB evolution. In spite of the large difference in their total mass, the ZAHB location (open circle in Fig. 5) of both models is quite similar and at $\log(L/L_\odot) \approx 2.4$ and $\log T_e \approx 3.6$. These values are a consequence of

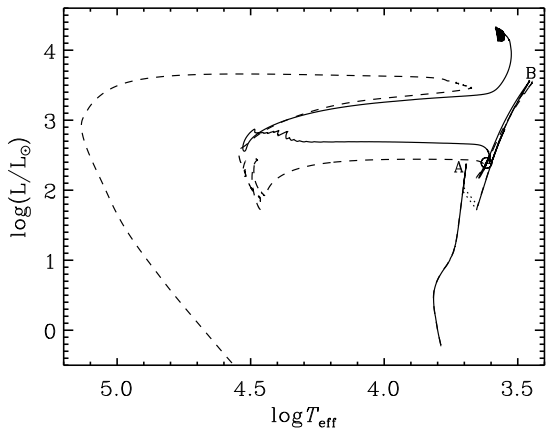

Fig. 5.— The H-R diagram of $0.82\,M_{\odot}$ models experiencing H-flashes, with Reimers' mass-loss ($\eta = 0.4$, dashed line) and without mass-loss (solid line). In Table 1 these models are denoted as B2 resp. B1. The open circle indicates the — almost identical — ZAHB-positions of the two models.

the H-flash which increases the surface metallicity ($Z_{\rm surf} \approx 0.017$) in both models. Therefore, they behave as metal-rich stars which are known to show quite red ZAHB location for masses larger than $\approx 0.55\,M_{\odot}$ (see for instance Bono et al. 1997). One notices that soon after the onset of core He burning both models perform an excursion toward the blue side of the H-R diagram. This behaviour can be explained by the quite large helium abundances in their envelopes ($Y_S \approx 0.5$).

The possibility that a metal-deficient stellar population produces a significant number of RR-Lyrae pulsators has been investigated by Cassisi et al. (1996). Neglecting the HEFM, the ZAHB location of metal-deficient stars is always hotter than the RR-Lyrae instability strip, and one cannot expect to have any ZAHB pulsators. In addition, a close inspection of the evolutionary paths in the H-R diagram revealed that the possibility to form a significant number of variables from the more evolved stars is negligible, too. In our scenario, accounting for the HEFM process and a subsequent H-flash, once again the possibility that metal-free stars produce RR-Lyrae variables is quite negligible, but for the opposite reason: metal-deficient HB stars experiencing the H-flash have ZAHB locations too red in comparison with the RR-Lyrae instability strip. In this respect, metal-deficient stars, the surface of which has been polluted during the H-flash phase, behave as "true" metal-rich stellar structures. The only possibility for obtaining ZAHB pulsators is a quite strong, but improbable mass-loss rate ($\eta_{\rm Reimers} > 0.4$), which 'forces' the ZAHB location to lie within the instability strip. The post ZAHB evolution does not yield an appreciable number of RR-Lyrae stars, because the instability strip is crossed in a very short time ($\approx 1-2$ Myr).

4.2. The helium shell-burning phase.

The high He abundance in the envelope of post H-flash stars ($Y \approx 0.5$) leads to a large burning rate in the H shell. Therefore, at the end of core He burning the size of the H-rich envelope is significantly reduced in comparison to models which did not experience the H-flash at the RGB tip. Hence the HB progeny of a formerly H-flashing star has a larger probability to evolve as AGB-manqué or post Early-AGB objects.

The evolution of low-mass metal-deficient stars during the Asymptotic Giant Branch (AGB) has been investigated by Cassisi et al. (1996) and Fujimoto et al. (2000). It was found that for these masses, a process quite similar to the HEFM discussed previously can occur at the beginning of the thermal-pulse phase. Hydrogen is mixed into the convective zone driven by He-burning, causing – like in the H-flash phase at the tip of the RGB – significant changes in the surface chemical composition.

Because we have evolved model B2 (no mass-loss) through the AGB phase we are now in the position to explore whether the H-flash at the RGB tip affects the AGB evolution. In Fig. 6 we show the evolution of the H-burning, the He-burning, and the total stellar luminosity during the first 8 thermal pulses of model B2. We have found an interesting, but expected result: if a H-flash occurred at the RGB tip, then the star behaves as a normal thermal pulsing Pop. I or II star with no further HEFM episode on the AGB.

This behaviour is due to the dredge-up of metals — carbon and nitrogen — into the stellar envelope during the H-flash phase, with the consequence that during the following AGB evolution the H-burning shell moves into a region no more

devoid of metals.

Before concluding this section we briefly discuss the carbon-oxygen (CO) abundance profile during the AGB phase. The CO stratification at this stage corresponds closely to that inside the final white dwarf configuration, which is a key parameter to determine its cooling time (see, e.g., Salaris et al. 1997). In Fig. 7 we show the carbon and oxygen profiles within the CO core at the 5th thermal pulse for our standard model (S1) and for a $1\,M_{\odot}$ star of solar composition. In spite of the very different initial metallicity, the CO profile is quite similar throughout the core, and moreover it is not affected by the occurrence of a H-flash during the RGB evolution of the standard model. A notable difference, however, is the extension (in mass) of the core itself. The standard model shows a much larger CO core, by about $0.1\,M_{\odot}$. This should correspond to an analogous difference for the final white dwarf masses, provided both structures leave the AGB after approximately the same number of pulses. We refrain from comparing in detail these profiles with corresponding results (for solar metallicity stars) by Salaris et al. (1997), because in our models we not only neglect semiconvection during the quiescent He-burning phase, but also use a different $^{12}C(\alpha,\gamma)^{16}O$ reaction rate.

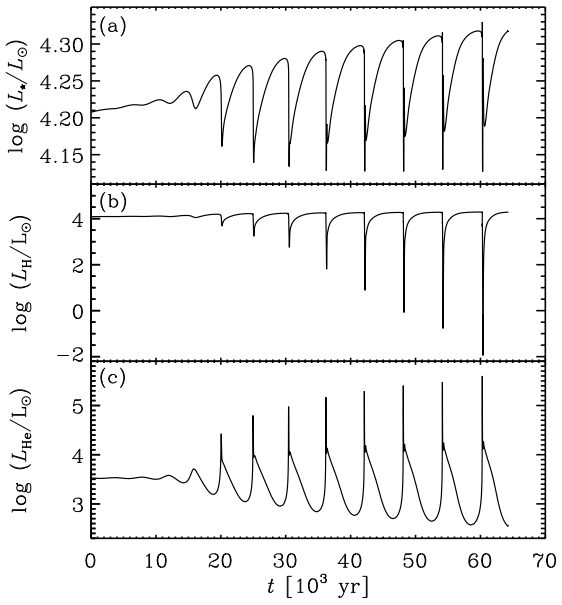

Fig. 6.— The evolution of the total (a), the H-burning (b), and the He-burning luminosity (c) during the first 8 thermal pulses on the AGB for model B2 (see Table 1); this model experienced a H-flash during the HEFM phase.

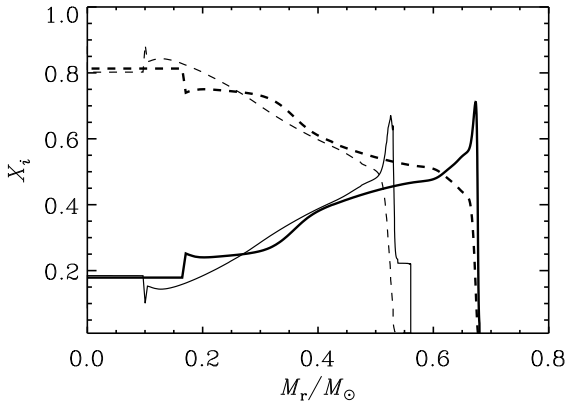

Fig. 7.— The chemical stratifications of carbon (solid) and oxygen (dashed line) within the core during the 5th thermal pulse for $1\,M_{\odot}$ models with two different initial chemical composition: metal-free (thick lines) and solar composition (thin lines).

5. Comparison with observations.

Our ultimate goal being to investigate the conjecture that the observed ultra-metal poor stars are the first low-mass stars in our Galaxy, we now confront our models with the observations. According to Beers (1999) 10% of the stars with [Fe/H] ≤ -2.5 show a carbon overabundance of [C/Fe] ≥ 1.0, this fraction rising to 25% at [Fe/H] ≤ -3.0, with the excess increasing to [C/Fe] $= 2$ at the lowest metallicities (Rossi et al. 1999). In addition, nitrogen is enhanced to similar levels (where determined), while oxygen remains normal with respect to iron, i.e. enhanced by ≈ 0.4 dex as is typical for Pop. II. No standard stellar source is known for producing such abundances (Timmes, Woosley, & Weaver 1995) and neither do so massive Pop. III supernovae (Heger & Woosley 2000; private communication). We therefore follow the idea that the peculiar C and N abundances stem from H and He burning in the interior, while all heavier elements are the result of pollution or accretion. Our first prediction therefore would be that only post He-flash objects

Table 2

Observational properties for some selected theoretical models and for two extremely metal-poor star.

Model	Age [Gyr]	$T_{\rm eff}$ [K]	$\log L/L_\odot$	[C/Fe]	[N/Fe]	[Fe/H]	$^{12}C/^{13}C$
CS22892-052	15.6 ± 4.6 (1)	4760 (2)	2.5[a]	1.1 (3)	1.0 (3)	-3.0 (3)	$\gtrsim 10$ (4)
CS22957-027	···	4840 (5)	1.7[b]	2.2 (4)	2.0 (4)	-3.4 (4)	10 (4)
B1	13.7	4500	1.71	3.9	4.1	-3.3	4.8
	13.7	4700	2.4	4.0	4.2	-3.3	4.4
B2	13.7	4450	1.77	3.8	4.0	-3.2	4.8
DP1	6.57	4570	1.68	2.2	2.5	-1.7	4.6

[a]Derived from $T_{\rm eff}$ and $\log g = 1.3$ of Reference (2) by assuming a mass of $0.82\,M_\odot$.

[b]Derived like for CS22892-052 from $\log g = 2.25$ of Reference (5)

References.—(1) Cowan et al. (1997); (2) Sneden et al. (1996); (3) Norris, Ryan, & Beers (1997a), (4) Norris, Ryan, & Beers (1997b); (5) Bonifacio, Molaro, Beers, & Vladilo (1998)

can show enhanced C and N abundances. Because the flash occurs at comparably low luminosities in Pop. III stars and the star experiences a rather long-lived second RGB phase at lower $T_{\rm e}$ (due to the strongly increased metal abundance in the envelope[10]), such stars can also be found at rather moderate RGB-brightness.

As a first object to compare with we chose CS22892-052, which is probably the best-observed star outside the solar system. In Table 2, we list the stellar properties. The effective temperature we took from (Sneden et al. 1996) as well as its gravity ($\log g = 1.5$). Assuming that the mass is that of our model star with the turn-off age being 13 Gyr ($0.82\,M_\odot$), we derive the luminosity to be $\log L/L_\odot \approx 2.5$. Additionally, we add CS22957-027 (Norris, Ryan, & Beers 1997b).

We compare these observed values with the ones obtained from our "best" models (B1 & B2), whose properties are listed in the next three rows of Table 2. We consider B1 and B2 to be the best theoretical counterparts of CS22892-052, since their mass is the one chosen to represent currently evolving Pop. III stars (their age at the RGB tip is 13.5 Gyr, consistent with actual estimates of the age of the Universe, and with the value for CS22892-052 obtained by Cowan et al. (1997) from nuclear chronology). From the B1-sequence we selected two models: the first one immediately after the helium flash and the second one at a luminosity as estimated for CS22892-052. The first one is also close to the luminosity of CS22957-027. These models are at the approximately correct locations in the HRD. We have tuned the amount of polluted matter in order to match approximately the observed [Fe/H] ratio in these stars. The predicted C and N abundance ratios with respect to iron are listed in Table 2, columns 5 and 6.

These theoretical predictions are 2–3 dex larger than the observed values. Even if there are objects at that metallicity that show enrichments in carbon of up to [C/Fe]=3, our models still predict too much carbon and nitrogen. In fact, while the observations indicate a spread in the overabundances, our models seem to produce always the same amount of C and N, such that [C/Fe] and [N/Fe] depend on the assumed pollution in Fe, which does, however, not influence the HEFM. Our models thus clearly fail to reproduce the absolute amount of carbon and nitrogen in these stars

[10]calling such post-flash stars *metal-poor* is appropriate if one refers to true metals only

and it remains to be investigated whether an additional parameter controlling C and N production can be found.

In Table 2 we list the same quantities also for a $1\,M_\odot$ model (DP1). It is evident that in this case the [C/Fe] and [N/Fe] ratios are in better agreement with observations, but this result is just due to the fact that this model was polluted with more material and therefore has a higher abundance of iron at the surface, which disagrees with the observed one. We add this model only to underline the fact that the amount of polluting material hardly influences the internal C and N production.

On the other side, it is reassuring that [C/N], which is 0.1 in CS22892-052 and 0.2 in CS22957-027, is similar in our models (≈ -0.2), and that effective temperature and luminosity can be matched with models after the He-flash.

6. Discussion and final remarks.

In the present work we have investigated the evolution of low-mass metal-free stars during the central ignition of He burning at the RGB tip. We have used an improved description of mixing and nuclear reaction network for these peculiar stellar structures. This has allowed us to examine in detail the occurrence and the properties of a mixing process induced by the He-flash.

Our results provide independent support for the conclusions reached by Fujimoto and coworkers. Actually, when the H-flash occurs, not only the general properties of this phenomenon, but also its final consequences on the surface chemical abundances, are quite similar to those found by Hollowell et al. (1990) and Fujimoto et al. (2000). There is an important difference, however: whereas they claim that the H-flash is a common property of all low-mass ($< 1.0\,M_\odot$) metal-deficient stars, we have found that the occurrence of a H-flash depends on the adopted initial conditions, like mass and He abundance, as well as on the assumptions made for the treatment of some physical process like diffusion and external pollution. Our computations disclose that the occurrence of a H-flash is mainly governed by one parameter: the position of the maximum He-burning energy release in the He-flash. The deeper inside the star this point lies, the lower is the probability that the convective zone developing at the He-flash ignition can penetrate into the hydrogen-rich envelope, thereby carrying down protons and triggering a H-burning runway.

A first comparison with CS22892-052 and CS22957-027 revealed a good match of effective temperature and luminosity and the relative abundances of carbon and nitrogen, but a severe overproduction of these elements, which is independent of the assumed amount and composition of the polluting material. Even if the H-flash phenomenon provides an interesting working scenario for interpreting the observed abundance patterns in extremely metal-deficient stars, it is not yet able to provide a detailed match to the observations. There are several possible interpretations of this failure, and we are now going to comment on some of them.

In the H-flash N is produced in the CN-chain by the fusion of carbon with hydrogen. Thus, any process destroying part of the carbon before the HEFM occurs also reduces the final nitrogen abundance. Obviously, with the rate of the $^{12}\mathrm{C}(\alpha,\gamma)^{16}\mathrm{O}$ reaction being affected by a large uncertainty (Buchmann 1996), a possible process to reduce the carbon abundance can be identified. However, our computations show that the mean temperature in the He-burning region is far too low for the $^{12}\mathrm{C}(\alpha,\gamma)^{16}\mathrm{O}$ reaction being efficient. Hence the demanded changes in the $^{12}\mathrm{C}(\alpha,\gamma)^{16}\mathrm{O}$-rate to process considerable amounts of carbon, would be much larger than the experimental uncertainties. In addition, the surface oxygen abundance would be increased considerably, in contrast to the observations, which reveal an oxygen content typical for Pop. II stars.

Another possibility for reducing the amount of C and N dredged up to the surface is an outward shift of the lower boundary of the convective zone driven by the H-flash, when merging with the convective envelope. It is however unclear how this could be done, because in all our models, even in the one containing the opacity with C-and N-enhanced mixture — which we consider to be the most reliable ones — the convective boundaries are located almost at the same position.

The third, and in our opinion the most promising way out of the high C and N abundances lies in an improvement of the crude one-dimensional description used to calculate the violent H burning in the HECZ zone. Possibly, we overestimate

the convective velocity, and thus the penetration depth of hydrogen. Model A1 with reduced velocities of the convective elements shows the tendency of smaller carbon and nitrogen abundances (about 30% less than in the standard model S1, cf. Table 1). In addition, the $^{12}C/^{13}C$-ratio, which in all H-flashing models is about 4.5 ± 0.5, is 5.6 in model A1, which again points toward the experimental value of $\gtrsim 10$. A similar result might be obtained if the penetration of the HECZ into the H-rich layers could be delayed until the temperature in the He-burning shell has diminished. We add that in the first two possibilities presented above the ingested hydrogen would be burnt under the same conditions yielding the same lower values for $^{12}C/^{13}C$.

Nevertheless, since the dredge-up of C and N to the surface is a consequence of the huge amount of energy released by hydrogen fusion, and thus by the production of nitrogen, a minimum value for the nitrogen abundance must exist. Below this value, the H-burning energy release is not sufficient to change the subsequent evolution of the star and no dredge-up would occur. Further investigations are required for deciding whether the observed N and C abundances can be reproduced by a modified mixing/burning description or by multidimensional simulations.

We point out a further potential problem that might become evident with larger samples of well-investigated metal-poor stars: since we predict carbon-enhancement due to internal production only during the He-flash, stars on the main sequence or near the turn-off should not display the same abundance pattern. In addition, above the post-flash luminosity ($\log L/L_\odot \approx 1.5$) the number of post-flash to pre-flash stars should reflect the evolutionary timescales (since the mass is approximately constant, assuming similar ages for all such halo stars); the ratio should be around 1:5 rising with increasing luminosity. This number is not too far from the observed numbers, but it is unknown to what extent observational biases might have influenced this. It is therefore extremely important to get larger samples with additional information about the stellar brightness.

Although our models face severe problems when comparing them to the best-observed ultra metal-poor star, CS22892-052, they still offer the only source for producing the observed C and N abundance patterns. Due to the mixing of protons into He-burning regions, *s*-process elements might result from the HEFM. We will investigate this and the evolution of light elements (^{7}Li) in future work.

This work was supported by a DAAD/VIGONI grant. One of us (S.C.) warmly thanks for the financial support by MURST (Cofin2000) under the scientific project: "Stellar observables of cosmological relevance". A.W. is grateful for the hospitality at the Institute for Advanced Study and Princeton Observatory and for a Fulbright fellowship which allowed visiting both places. Helpful discussions with T. Beers, C. Sneden, J. Cowan and J. Truran and the very careful reading of the manuscript by H. Ritter are acknowledged.

REFERENCES

Alexander, D. R. & Fergusson, J. W. 1994, ApJ, 437, 879

Beers, T. C. 1999, in Astrophy. and Space Science, Vol. 265, Connecting the Distant Universe with the Local Fossil Record, ed. M. Spite (Dordrecht: Kluwer Academic Publishers), 547

Beers, T. C., Preston, G. W., & Shectman, A. 1992, AJ, 103, 1987

Bond, H. E. 1980, ApJS, 44, 517

Bonifacio, P., Molaro, P., Beers, T. C., & Vladilo, G. 1998, A&A, 332, 672

Bono, G., Caputo, F., Cassisi, S., Castellani, V., & Marconi, M. 1997, ApJ, 479, 279

Buchmann, L. 1996, ApJ, 468, L127

Canuto, M. & Mazzitelli, I. 1991, ApJ, 370, 295

—. 1992, ApJ, 389, 724

Cassisi, S. & Castellani, V. 1993, ApJS, 88, 509

Cassisi, S., Castellani, V., & Tornambé, A. 1996, ApJ, 459, 298

Castellani, V. 2000, in MPA/ESO workshop: The First Stars, ed. A. Weiss, T. Abel, & V. Hill (Heidelberg: Springer), 85

Chiosi, C. 2000, in MPA/ESO workshop: The First Stars, ed. A. Weiss, T. Abel, & V. Hill (Heidelberg: Springer), 95

Cowan, J. J., Pfeiffer, S. G., Kratz, K.-L.., Tielemann, F.-K.., Sneden, C., Burles, S., Tytler, D., & Beers, T. C. 1997, ApJ, 521, 194

Fujimoto, M. Y., Iben, I. jr., & Hollowell, D. 1990, ApJ, 349, 580

Fujimoto, M. Y., Ikeda, Y., & Iben, I. jr. 2000, ApJ, 529, L25

Hill, V. et al. 2000, A&A, 353, 557

Hollowell, D., Iben, I. jr., & Fujimoto, M. Y. 1990, ApJ, 351, 245

Iglesias, C. A. & Rogers, F. J. 1996, ApJ, 464, 943

Itoh, N., Mitake, S., Iyetomi, H., & Ichimaru, S. 1983, ApJ, 273, 774

Kippenhahn, R. & Weigert, A. 1990, Stellar Structure and Evolution (Berlin, Heidelberg: Springer-Verlag)

Kippenhahn, R., Weigert, A., & Hofmeister, E. 1967, Methods in Computational Physics, Vol. 7, Methods for Calculating Stellar Evolution (New York: Academic Press), 129

Langer, N., El Eid, M., & Fricke, K. J. 1985, A&A, 145, 179

Munakata, H., Kohyama, Y., & Itoh, N. 1985, ApJ, 296, 197

Norris, J. E., Ryan, S. G., & Beers, T. C. 1997a, ApJ, 488, 350

—. 1997b, ApJ, 489, L169

Reimers, D. 1975, Mem. Soc. Roy. Sci. Liège, 8, 369

Rogers, F. J., Swenson, F. J., & Iglesias, C. A. 1996, ApJ, 456, 902

Rossi, S., Beers, T. C., & Sneden, C. 1999, in ASP Conf. Ser., Vol. 165, The Third Stromlo Symposium: The Galactic Halo, ed. T. A. B.K. Gibson & M. Putma (San Francisco: ASP), 264

Salaris, M., Dominguez, I., García-Berro, E., Hernanz, M., Isern, J., & Mochkovitch, R. 1997, ApJ, 486, 413

Schlattl, H. 1999, Ph.D. thesis, Technical University Munich

—. 2000, Phys. Rev. D, submitted

Schlattl, H. & Weiss, A. 1999, A&A, 347, 272

Sneden, C., McWilliam, A., Preston, G. W., Cowan, J. J., Burris, D. L., & Armosky, B. J. 1996, ApJ, 467, 819

Thoul, A. A., Bahcall, J. N., & Loeb, A. 1994, ApJ, 421, 828

Timmes, F. X., Woosley, S. E., & Weaver, T. A. 1995, ApJS, 98, 617

Vitense, E. 1953, Z. Astrophys., 32, 135

Wagenhuber, J. 1996, Ph.D. thesis, Technical University Munich

Wagenhuber, J. & Weiss, A. 1994, A&A, 286, 121

Weiss, A., Cassisi, S., Schlattl, H., & Salaris, M. 2000, ApJ, 533, 413

Weiss, A. & Schlattl, P. 2000, A&A Suppl., 144, 487

Yoshii, Y. 1981, A&A, 97, 280

This 2-column preprint was prepared with the AAS LaTeX macros v5.0.